

## ANALYSIS OF THE CONTRIBUTION DEGREE OF VIBRATION TRANSMISSION OF BOLTED STRUCTURE

SHUAI LIU

*Harbin Engineering University, Harbin, China; and  
Science and Technology on Reactor System Design Technology Laboratory, Chengdu, China  
e-mail: liushuai\_9105@163.com*

WANYOU LI

*Harbin Engineering University, Harbin, China*

XUAN HUANG, FURUI XIONG, XIAOZHOU JIANG, ZHIPENG FENG,  
LIWEI DENG, ZHIHAO YUAN, GUOJIANG LIAO, WANJUN WU

*Science and Technology on Reactor System Design Technology Laboratory, Chengdu, China*

In practical engineering, vibration transmission between bolted structures supported by cantilever beams involves many factors. The vibration transmission effect is the embodiment of coupling of various factors, so it is impossible to accurately and quantitatively evaluate the influence degree of various factors. In this paper, the influence factors of vibration between bolted plates in the form of a cantilever beam are studied by a numerical calculation method. The effects of the friction coefficient, bolt preload, temperature and pressure on vibration characteristics are studied. Finally, the contribution of different influencing factors to vibration transmission is given.

*Keywords:* bolted structures, vibration transmission, numerical calculation

### 1. Introduction

Bolt connection is a common connection form in large assemblies, which is widely used in mechanical structures such as nuclear power equipment. In numerical simulation of dynamic characteristics of mechanical structures, different models of bolted connection (Rogers and Boothroyd, 1975; Du *et al.*, 2018; Shen *et al.*, 2020) have a great influence on the process and results of numerical simulations. In a submersible interior, a power device is connected to the base through a support which is usually connected by elastic or bolt connection. In the environment of a deep sea, when connection with the base is by bolts, transmission of structural vibration (Tullini and Laudiero, 2008; Li *et al.*, 2017; Hao *et al.*, 2021) is affected by many factors, including the fit of bolts and holes, friction between the plate and plate joint surfaces, deformation of the shell base, etc. Simulation of vibration transmission under bolted connection is complex. The vibration transmission mechanism and simulation modes are not clear, which needs to be further studied. In this paper, vibration transmission between a submersible internal structure and the base is studied. The model of bolted connection is established and the influencing factors of vibration transmission are studied. The law of vibration of typical bolted connection is given from the perspective of numerical simulation, which can be used as a reference for design.

## 2. Simulation model of bolted connection

### 2.1. Geometric model

Taking a bolted plate structure as an example, the influence of various models of bolted connection on dynamic characteristics of the example is studied. By analysing the bolted structure, nonlinear factors mainly exist in the connection position. The friction coefficient, preload, temperature, pressure can lead to a change of vibration transmission in bolt connection. So the influence laws of the friction coefficient, preload, temperature, pressure and other parameters are studied. Combined with a vibration experimental model of the bolted plate structure, suggestions for numerical simulation mode and vibration transmission contribution of the bolted plate structure are given. The bolt connection mechanism model established in this paper is shown in Fig. 1.

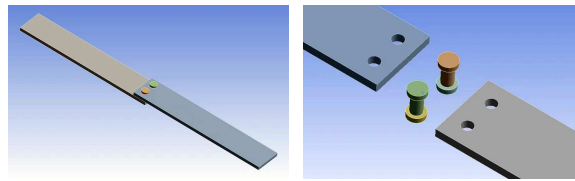


Fig. 1. The bolted plate

### 2.2. Size and coordinates of the model

The size of the flat plate is  $200\text{ mm} \times 40\text{ mm} \times 5\text{ mm}$  (overlapping length is 20 mm). The diameter of the through hole at the connection is 6.5 mm and the diameter of the contact circle between the end face of the bolt or nut and the flat plate is about 10 mm. Both the flat plate and the bolt are made of steel, as shown in Fig. 2.

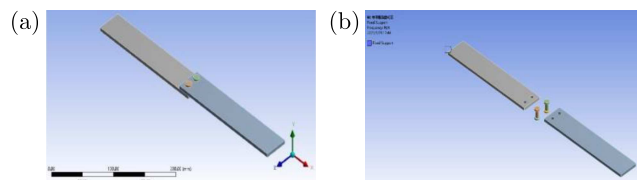


Fig. 2. Size and coordinates of the model: (a) coordinate, (b) boundary conditions

The coordinate system:  $X$  axis is along the length direction,  $Y$  axis is along the thickness direction, and  $Z$  axis is along the width direction of the plate. Rigid fixed constraints are adopted at one end of the length direction.

## 3. Research on simulation model

In order to obtain a proper simulation method of the bolted connection, different simulation methods are discussed. The bolt connection structure is complex, and it is inefficient to it in large and complex structures. Therefore, the bolt connection structure is usually reasonably simplified. This paper mainly studies the following five simplified models to explore the influence of the bolt simulation mode on structural dynamic characteristics when the bolted flat plate structure is connected. In the paper, the bolt is simulated by making use of five following elements:

- 1) Unthreaded solid element;
- 2) Cylinder solid element;
- 3) Byline element;

- 4) Beam element;
- 5) Joint element.

Referring to the five simplified models and distinguishing details in the model, the following 12 calculation models are established to analyze dynamic characteristics of bolted structures.

- Model 1A: unthreaded solid model with bonded contact, as shown in Fig. 3a;
- Model 1B: unthreaded solid model with nodes of the contact surface combined (Fig. 3b);
- Model 2A: cylinder solid model with bonded contact (Fig. 4a);
- Model 2B: cylinder solid model with nodes of the contact surface combined (Fig. 4b);
- Model 3A: line element with contact (beam constraint) (Fig. 5a);
- Model 3B: line element with MPC contact (multipoint constraint) (Fig. 5b);
- Model 4A: beam element with stress on the through-hole cylinder face (Fig. 6a);
- Model 4B: beam element with stress on the through-hole sideline (Fig. 6b);
- Model 4C: beam element with stress on the bolt contact surface (Fig. 6c);
- Model 5A: joint connection with stress on the through-hole cylinder face (Fig. 7a);
- Model 5B: joint connection with stress on the through-hole cylinder sideline (Fig. 7b);
- Model 5C: joint connection with stress on the bolt contact surface (Fig. 7c).

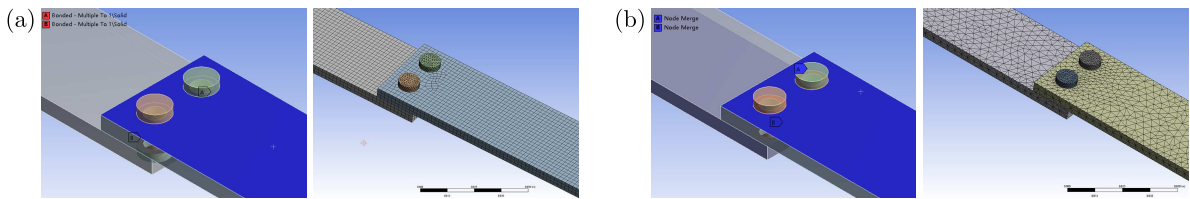


Fig. 3. Model 1A (a) and model 1B (b)

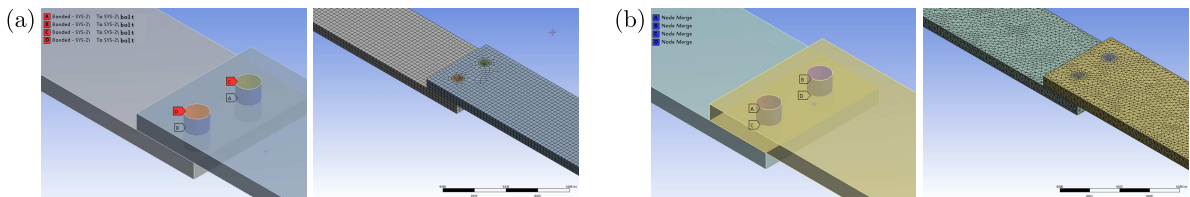


Fig. 4. Model 2A (a) and model 2B (b)

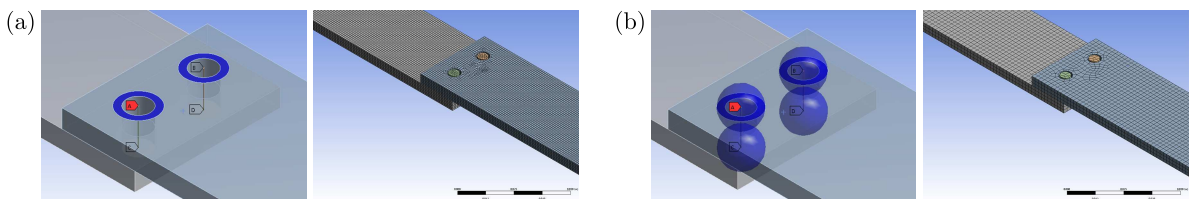


Fig. 5. Model 3A (a) and model 3B (b)

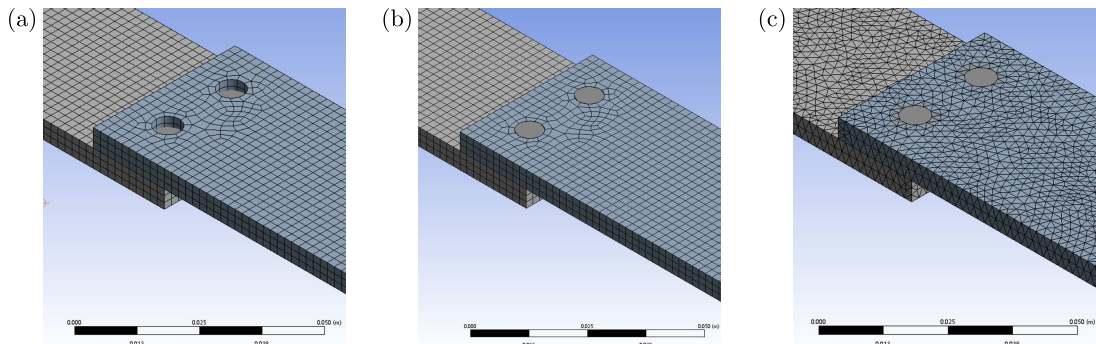


Fig. 6. Model 4A (a), model 4B (b) and model 4C (c)

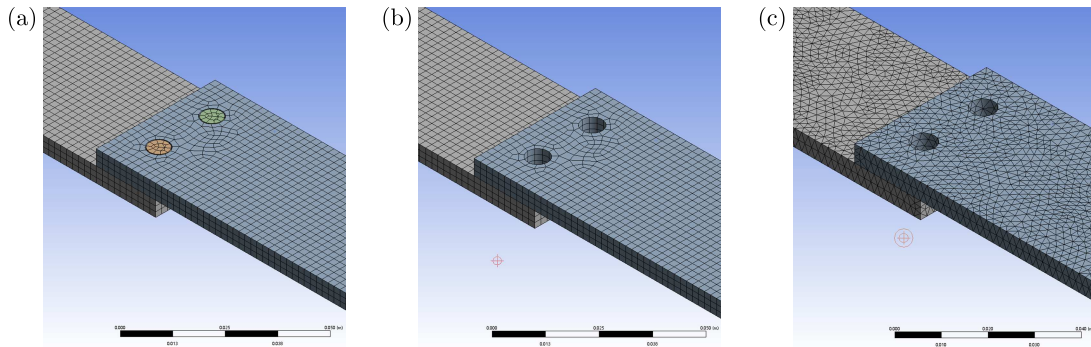


Fig. 7. Model 5A (a), model 5B (b) and model 5C (c)

## 4. Modal theory

### 4.1. Modal analysis theory

The essence of modal analysis is a coordinate transformation. Its purpose is to put the response vector originally described in the physical coordinate system into the so-called "modal coordinate system". Each basis vector of this coordinate system is just an eigenvector of the vibration system. In other words, in this coordinate, the vibration equation is a set of equations without coupling with each other, which respectively describe vibration forms of each order of the vibration system. Each coordinate can be solved separately to obtain a certain order of structural parameters of the system.

After discretization, the dynamic characteristics of the structure can be described by  $n$ -order matrix differential equation

$$\mathbf{M}\ddot{\mathbf{x}} + \mathbf{C}\dot{\mathbf{x}} + \mathbf{K}\mathbf{x} = \mathbf{f}(t) \quad (4.1)$$

where  $\mathbf{M}$ ,  $\mathbf{K}$  and  $\mathbf{C}$  are the mass, stiffness and damping matrix of the structure,  $\mathbf{x}$ ,  $\dot{\mathbf{x}}$  and  $\ddot{\mathbf{x}}$  are  $n$ -displacement, velocity and acceleration response vectors,  $\mathbf{f}(t)$  is the  $n$ -dimensional excitation force vector.

Assuming that the initial state of the system is zero, the matrix equation with a complex  $s$  variable (Eq. (4.2)) can be obtained by the Laplace transformation on both sides of Eq. (4.1)

$$[\mathbf{M}s^2 + \mathbf{C}s + \mathbf{K}]\mathbf{X}(s) = \mathbf{F}(s) \quad (4.2)$$

The matrix in the formula is

$$\mathbf{Z}(s) = [\mathbf{M}s^2 + \mathbf{C}s + \mathbf{K}] \quad (4.3)$$

It reflects the dynamic characteristics of the system, which is the system dynamic matrix or impedance matrix. Its inverse matrix is

$$\mathbf{H}(s) = [\mathbf{M}s^2 + \mathbf{C}s + \mathbf{K}]^{-1} \quad (4.4)$$

$\mathbf{H}(s)$  is the admittance matrix, that is, transfer function matrix. According to Eq. (4.2)

$$\mathbf{X}(s) = \mathbf{H}(s)\mathbf{F}(s) \quad (4.5)$$

Set  $s = j\omega$  in Eq. (4.5), the relationship between the output (response vector  $\mathbf{X}(\omega)$ ) and input (excitation vector  $\mathbf{F}(\omega)$ ) in the frequency domain can be obtained

$$\mathbf{X}(\omega) = \mathbf{H}(\omega)\mathbf{F}(\omega) \quad (4.6)$$

where  $\mathbf{H}(\omega)$  is the frequency response function matrix. The elements in rows and columns of the matrix  $\mathbf{H}(\omega)$  are

$$H_{ij}(\omega) = \frac{X_i(\omega)}{F_j(\omega)} \quad (4.7)$$

Set  $s = j\omega$  in Eq. (4.3), the impedance matrix can be obtained

$$\mathbf{Z}(\omega) = (\mathbf{K} - \omega^2\mathbf{M}) + j\omega\mathbf{C} \quad (4.8)$$

Using the weighted orthogonality of a real symmetric matrix, matrix equations are obtained

$$\Phi^T \mathbf{M} \Phi = \begin{bmatrix} \ddots & & & \\ & m_r & & \\ & & \ddots & \\ & & & \ddots \end{bmatrix} \quad \Phi^T \mathbf{K} \Phi = \begin{bmatrix} \ddots & & & \\ & k_r & & \\ & & \ddots & \\ & & & \ddots \end{bmatrix} \quad (4.9)$$

The matrix  $\Phi = [\phi_1, \phi_2, \dots, \phi_N]$  is the vibration mode matrix, and it is assumed that the damping matrix also satisfies the orthogonality of vibration modes

$$\Phi^T \mathbf{C} \Phi = \begin{bmatrix} \ddots & & & \\ & c_r & & \\ & & \ddots & \\ & & & \ddots \end{bmatrix} \quad (4.10)$$

Substitute equation (4.10) into equation (4.8), equation (4.11) is obtained

$$\mathbf{Z}(\omega) = \Phi^{-T} \begin{bmatrix} \ddots & & & \\ & z_r & & \\ & & \ddots & \\ & & & \ddots \end{bmatrix} \Phi^{-1} \quad (4.11)$$

where  $z_r = (k_r - \omega^2 m_r) + j\omega c_r$

$$H_{ij}(\omega) = \sum_{r=1}^N \frac{\phi_{ri} \phi_{rj}}{m_r [(\omega_r^2 - \omega^2) + j2\xi_r \omega_r \omega]} \quad (4.12)$$

#### 4.2. Modal test theory

The connection between the steel plate and the bolt is a continuous structural system, but in vibration modal tests and analysis, it can only be described as a finite degree of freedom system. In the frequency band of interest, such as  $(f_a, f_b)$ , according to the complex mode theory, the frequency response function of the structure can be expressed as

$$H_{ij}(\omega) = \frac{1}{2} \sum_{k=k_a}^{k_0} \left[ \frac{r_{ijk} e^{\theta_{ijk}}}{(\omega_k - \omega) + i\sigma_k} - \frac{r_{ijk} e^{-\theta_{ijk}}}{(\omega_k - \omega) - i\sigma_k} \right] + R_{ij} = R_{ij} + \sum_{k=k_a}^{k_0} h_{ijk}(\omega) \quad (4.13)$$

where  $h_{ijk}(\omega)$  is the  $k$ -th order single-mode expression,  $R_{ij}$  stands for the residual term of the frequency band.  $k_0, k_a$  are the lowest and highest modal orders in the  $(f_a, f_b)$  frequency band.  $\sigma_k, \omega_k, r_{ijk}$  and  $\theta_{ijk}$  are the damping coefficient of the  $k$ -th mode, damped natural frequency and amplitude, and the amplitude of the vibration mode vector component generated at the point  $i$  when the excitation force is applied at the point  $j$ . Equation (4.13) shows that the measured frequency response is the superposition of various modes.

The coupling between the total vibration of the steel plate and bolt connection is weaker than that of the lower modes. Therefore, it can be considered that the measured frequency response function is only the contribution near the modal frequency, and the influence of the adjacent modes can be neglected. According to the assumption of the single freedom model, the frequency response function is reduced to the form

$$h_{ijk}(\omega) = \frac{r_{ijk}}{\Omega_k^2 - \omega^2 + 2i\xi_k\Omega_k\omega} \quad (4.14)$$

where  $\xi_k = \sigma_k/\Omega_k$  is the damping ratio;  $\Omega_k = \sqrt{\sigma_k^2 + \omega_k^2}$  is the undamped natural frequency.

In this test, if the pickup signal of the response is acceleration, then

$$h_{ijk}(\omega) = \frac{-\omega^2 r_{ijk}}{\Omega_k^2 - \omega^2 + 2i\xi_k\Omega_k\omega} \quad (4.15)$$

From frequency response function (4.15)

$$\begin{aligned} \operatorname{Re}[h_{ijk}(\omega)] &= \frac{-\omega^2(\Omega_k^2 - \omega^2)r_{ijk}}{(\Omega_k^2 - \omega^2)^2 + (2i\xi_k\Omega_k\omega)^2} \\ \operatorname{Im}[h_{ijk}(\omega)] &= \frac{2i\xi_k\Omega_k\omega^3 r_{ijk}}{(\Omega_k^2 - \omega^2)^2 + (2i\xi_k\Omega_k\omega)^2} \\ |h_{ijk}(\omega)| &= \frac{\omega^2 r_{ijk}}{(\Omega_k^2 - \omega^2)^2 + (2i\xi_k\Omega_k\omega)^2} \end{aligned} \quad (4.16)$$

After the measured frequency response function is obtained, the real frequency, imaginary frequency and amplitude frequency curves can be obtained at the same time. From Eq. (4.16)<sub>1</sub>, when  $\omega = \Omega_k$ ,  $\operatorname{Re}[h_{ijk}(\omega)]$  takes the zero value. In  $\omega = \Omega_k$ , Eqs (4.16)<sub>2</sub> and (4.16)<sub>3</sub> is the mean value. It can be seen that after measuring the frequency response function curve, each order of the frequency is very easy to obtain.

$\operatorname{Re}[h_{ijk}(\omega)]$  calculates the derivative, and making it zero one obtains the two extreme point frequencies near the zero value frequency (modal frequency) on the real frequency curve  $\omega_a$ ,  $\omega_b$  ( $\omega_a > \omega_b$ )

$$\omega_a^2 = \frac{\Omega_k^2}{1 + 2\xi_k} \quad \omega_b^2 = \frac{\Omega_k^2}{1 - 2\xi_k} \quad (4.17)$$

The above two equations are combined to find the damping ratio

$$\xi_k = \frac{(\omega_b/\omega_a)^2 - 1}{2[(\omega_b/\omega_a)^2 + 1]} \quad (4.18)$$

The vibration mode vector component of the  $k$ -th mode is obtained by the following equation

$$\phi_k = \{\operatorname{Im}[h_{ijk}(\omega)]\} \quad (4.19)$$

## 5. Modal numerical analysis

According to the above, the modal analysis of the bolted structure is completed, and the results are listed in Table 1. The corresponding vibration modes are shown in Figs. 8 and 9. We can get the natural frequency when the right end of formula (4.1) is 0.

Since deformation of vibration modes calculated by different models are similar, the mode of each order for 1B model are given as Figs. 8 and 9.

**Table 1.** The natural frequency of the bolted plate structure

Model	One end rigid fixed frequency [Hz]				Rigid fixed at both ends [Hz]			
	First	Second	Third	Fourth	First	Second	Third	Fourth
1A	27.14	172.10	212.26	494.49	171.72	569.35	956.20	965.80
1B	28.26	175.75	219.01	494.98	174.50	575.32	968.42	979.57
2A	28.20	173.37	213.18	494.62	173.64	569.80	960.59	976.59
2B	28.32	177.15	219.49	494.93	176.46	574.96	977.58	984.01
3A	28.35	177.81	219.84	494.89	177.21	574.98	979.34	986.85
3B	28.44	178.37	219.73	496.73	177.78	574.49	982.62	986.41
4A	28.25	174.56	205.64	494.66	174.88	564.25	966.80	979.57
4B	28.17	161.14	172.45	492.25	172.96	534.09	895.70	955.41
4C	28.14	172.09	203.09	494.54	171.75	559.27	956.13	969.09
5A	28.23	174.26	216.37	494.65	174.71	571.34	965.56	974.48
5B	28.23	173.78	189.03	494.52	174.46	541.12	961.27	981.99
5C	28.28	175.20	213.82	494.66	175.78	565.08	969.43	982.49

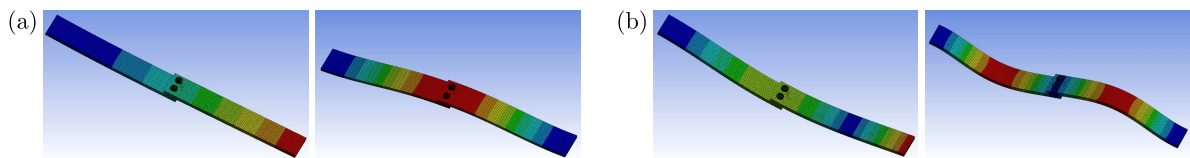


Fig. 8. (a) First order mode, (b) second order mode: left – one end fixed, right – two ends fixed

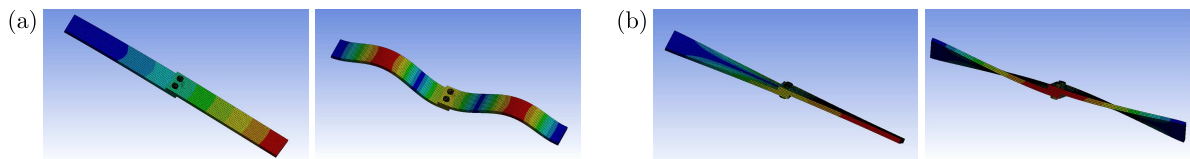


Fig. 9. (a) Third order mode, (b) fourth order mode: left – one end fixed, right – two ends fixed

The solid element can simulate more rich information. From the calculation results, it can be seen that the solid elements have little difference, so it can be inferred that the solid model adopted by the bolt is the closest model to the real structure. And the calculation results are the most accurate. However, the grid scale is much larger, especially when there are many bolts, the grid scale increases significantly, and the grid scale directly determines computational efficiency. When the grid scale is the same and there are many contacts, the computational efficiency is lower than that of node merging. When the elements and nodes are numerous, the bolt is recommended to be simplified by line or beam elements, and the bolt contact surface is set to stress surface, which can reduce the scale of the finite element model, improve calculation efficiency and high simulation accuracy. Using the simplified methods to simulate bolts can also ensure their quality and stiffness characteristics. Line or beam elements can simulate the quality and stiffness characteristics. From the natural frequency error calculated, we can see the error is small. For the bolt connection of two flat plates, the solid unthreaded element is adopted to analyse the impact of the parameters on dynamic characteristics.

The local structure of the bolted connection is free from structural deformation caused by external pressure in the deep-sea environment. Therefore, the main factors affecting vibration of bolted structures include friction, external pressure and temperature. Friction is reflected by different preloads. As depth of a deep sea varies, the external pressure and temperature on bolted structures vary with depth. This paper focuses on the influencing factors in 5.1-5.3. When

friction, pressure, temperature and bolt preload are loaded on the right end of formula (4.1), we can get results under different conditions.

### 5.1. The effect of the friction coefficient on vibration transmission

Based on model 1B, the influence of the friction coefficient on dynamic characteristics of the bolted plate structure is studied by two restraint methods:

Model F1: one end is rigidly fixed, the bolt is in contact with the upper and lower surfaces of the plate, and the upper and lower plates are in contact, the preload is 0;

Model F2: two ends are rigidly fixed, the bolt is in contact with the upper and lower surfaces of the plate, and the upper and lower plates are in contact, the preload is 0.

The change of natural frequencies of each order with the friction coefficient is calculated, which is listed in Table 2.

**Table 2.** Calculation results of models F1 and F2

Friction coefficient	F1 natural frequency [Hz]				F2 natural frequency [Hz]			
	First	Second	Third	Fourth	First	Second	Third	Fourth
0.02	27.70	160.65	194.20	483.99	162.78	559.09	880.94	963.95
0.10	27.92	165.66	197.72	486.60	165.80	560.52	905.38	964.16
0.20	27.95	166.34	199.81	487.56	166.25	561.62	909.23	964.26
0.90	28.00	167.60	208.29	490.93	165.35	564.00	902.18	964.41

Automatic adjustment of contact with structural deformation can be realized by the penalty function method. Through a change in the natural frequency with the friction coefficient, it can be seen that bolted plates become a fixed overall structure and the stiffness changes little with the friction coefficient. The natural frequency of each order increases with an increase of the friction coefficient.

### 5.2. The effect of bolt preload on vibration transmission

Based on model 1B, the friction coefficient is taken as 0.2 to study the influence of preload on the dynamic characteristics of the bolted plate structure:

Model P1: one end is rigidly fixed, the bolt is in contact with the upper and lower surfaces of the plate and the upper and lower plates are in contact. The friction coefficient is 0.2.

The law of natural frequencies of each order of the bolted structure with preload calculated are listed in Table 3.

**Table 3.** Calculation results of model P1

Preload	Natural frequency [Hz]			
	First	Second	Third	Fourth
2550 N	28.01	169.16	209.83	492.91
4200 N	28.02	169.17	209.83	492.94
6750 N	28.02	169.19	209.83	492.97
9000 N	28.03	169.21	209.86	493.04
13200 N	28.03	169.23	209.91	493.10
15500 N	28.04	169.27	209.95	493.14

The analysis shows that the two flat plates connected by bolts become a fixed overall structure. Its stiffness does not change much with the preload, and the natural frequency of each order increases with an increase of preload, but the change is not obvious.

### 5.3. The effect of temperature on vibration transmission

Based on model 1B, the influence of temperature on dynamic characteristics of bolted plates is studied, and the following two calculation models are established.

Model T1: one end is rigidly fixed, the bolt is in contact with the upper and lower surfaces of the plate, the upper and lower plates are in contact. The friction coefficient is 0.2 and the preload is 4200 N.

Model T2: two ends are rigidly fixed, the bolt is in contact with the upper and lower surfaces of the plate, the upper and lower plates are in contact. The friction coefficient is 0.2 and the preload is 4200 N.

According to calculations, the change of each order natural frequency with temperature is listed in Table 4.

**Table 4.** Calculation results of model T1 and T2

Temperature	T1 natural frequency [Hz]				T2 natural frequency [Hz]			
	First	Second	Third	Fourth	First	Second	Third	Fourth
100°C	27.88	167.20	207.83	492.03	69.42	468.10	839.41	955.32
22°C	28.03	169.25	209.94	493.10	169.54	566.76	939.27	964.93
10°C	28.04	169.50	210.34	493.43	178.34	578.20	943.49	966.13
0°C	28.05	169.71	210.97	493.78	185.18	587.03	945.75	967.10
-10°C	28.05	169.93	212.00	494.14	191.97	596.14	956.07	968.12
-20°C	28.06	170.11	212.63	494.35	198.57	605.07	964.00	969.16
-30°C	28.06	170.14	212.72	494.35	204.88	614.45	970.18	971.95
-50°C	28.07	170.19	213.82	494.92	217.45	632.18	972.32	992.06

The calculation results show that the influence of temperature on the frequency change is related to the connection form of the structure and boundary conditions. For the rigid fixed boundary condition at one end, it is equivalent to a cantilever beam. When temperature changes, its structure can expand or contract freely, and its internal stress (stiffness) changes little. Although the natural frequencies of each order decrease with an increase of temperature, the change is not obvious. For the rigid fixed boundary conditions at both ends, the connection form is equivalent to the rigid fixed beam. When temperature changes, the structure cannot expand freely. The temperature stress will be generated inside, which will affect the structural stiffness. The natural frequencies of each order decrease with an increase of temperature, and the change is obvious. When temperature drops from 22°C to -50°C, the first natural frequencies increase by about 5%-28%.

### 5.4. The effect of pressure on vibration transmission

Based on model 1B, the following is established:

Model N1: one end is rigidly fixed, the bolt is in contact with the upper and lower surfaces of the plate, the upper and lower plates are in contact. The friction coefficient is 0.2, preload 4200 N and temperature 22°C.

The change of natural frequencies of each order of the bolted structure with pressure is shown in Table 5.

The calculation results show that the two flat plates connected by bolts become a fixed overall structure, so stiffness changes little with pressure. The natural frequencies of each order increase with an increase of water depth, but the change is not obvious.

**Table 5.** Calculation results of model N1

Depth	Natural frequency [Hz]			
	First	Second	Third	Fourth
50 m	28.04	169.70	210.98	493.78
100 m	28.05	169.70	210.99	493.80
150 m	28.05	169.70	211.00	493.80
200 m	28.05	169.70	211.02	493.81
250 m	28.05	169.71	211.05	493.83
300 m	28.05	169.71	211.08	493.83

## 6. Comparison between calculations and tests

### 6.1. Test device

In order to study the influence of bolted plates on structural vibration transmission characteristics, the paper completes the modal test.

A cantilever beam is used to complete vibration modal analysis of bolted connection and fit. The experimental beam is made of steel. As shown in Fig. 10, the size of two steel plates is  $200\text{ mm} \times 40\text{ mm} \times 5\text{ mm}$ , which are steel plates 1 and 2, respectively. The left side of steel plate 1 is rigidly fixed to restrict the translational and rotational degree of freedom. The overlap length between steel plates is  $20\text{ mm}$ . The whole test piece is connected to the column and fixed on the large stiffness base by means of bolt connection. The test device and location of measuring points are shown in Fig. 10. The FEA testing tool is commercial. It is the special vibration testing tool of the Brüel&Kjær, named PULSE.

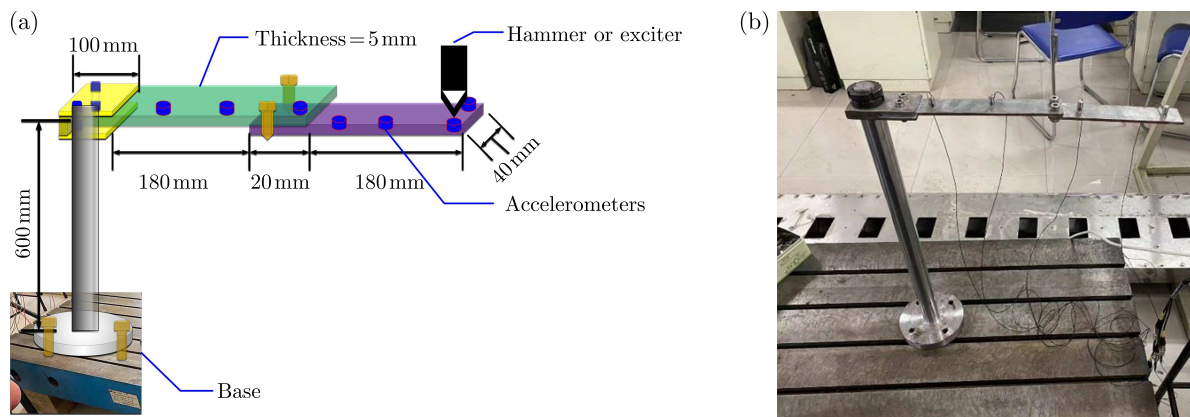


Fig. 10. Test device: (a) schematic diagram, (b) actual lab stand

The structural modal test of the cantilever beam is carried out through Jiangsu Dong Hua DH5922D data collector and Japan Riyin PV-91CH acceleration sensor. Because the length to width ratio of the cantilever beam is large, the test model is simplified to a beam element.

### 6.2. Comparison analysis

In the test, vertical first-order, vertical second-order and vertical third-order vibration modes appear, followed by a torsional first-order mode. The vibration modes are consistent with the numerical simulation results. The modal test results are as follows:

Through the change of bolt preload of the cantilever beam structure, the simulation results are compared with the experimental ones. Table 6 shows the test results of fit bolts under different preloads. The fit bolts in real connections are also preloaded.

**Table 6.** Comparison of frequency from simulations and tests

	Preload [N]	Natural frequency [Hz]			
		First	Second	Third	Fourth
Calculation	2550	28.01	169.16	209.83	492.91
	4200	28.02	169.17	209.83	492.94
	6750	28.02	169.19	209.83	492.97
Test	2550	24.414	140.365	180.624	362.305
	4200	24.414	141.602	181.439	379.883
	6750	24.414	141.602	182.001	380.654
Max difference [%]		14.7	20.5	16.2	36.0

Since the bolt preload has little effect on the natural frequency, the numerical calculation results for preload 2550 N are compared with the experimental results. The relative difference of the first-order natural frequency value is 14.7%, the second-order one 20.5%, third-order 16.2% and the fourth-order 36%. The first-order, second-order and third-order vertical mode appear firstly in the numerical simulation, followed by the first-order torsional mode, the same law as in experiment. And the change trend of the corresponding natural frequency value is roughly the same.

In the beam, the natural frequency is  $\omega = \sqrt{k/m}$ , where  $k$  is the stiffness coefficient and  $m$  is the structural mass. The experimental value is higher than that from numerical simulation, because when the boundary conditions are applied, the simulation can reach the stiffness of the cantilever beam, while the actual cantilever beam will not reach the ideal boundary conditions. In reality, the stiffness and natural frequency of the overall beam are reduced. The single mass of the acceleration sensor used in this experiment accounts for 0.46%. Four sensors are used, which makes the mass increase a little which, in turn, may reduce the natural frequency a little.

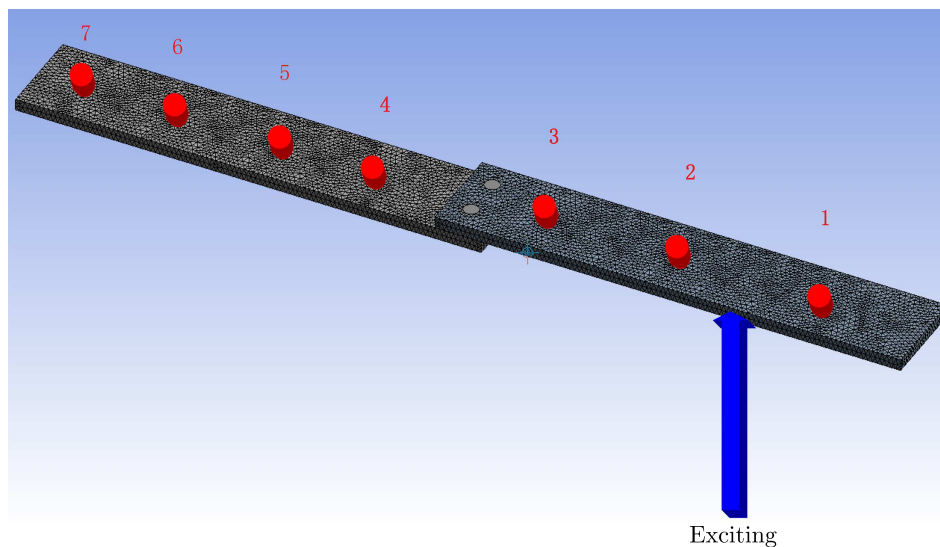


Fig. 11. Vibration response test points

The vibration response between simulation and test has been contrasted. In order to obtain more obvious vibration phenomena, the excitation with the same resonant frequency as the structure is used, so a force with a smaller excitation amplitude can also be used to obtain more obvious vibration phenomena. The response points are shown in Fig. 11. Applying a force with an amplitude of 1N at the exciting point and changing excitation frequencies, the vibration response at different points is obtained. Comparing the vibration response of point 3 and 4

under different preloads, the vibration change after transmission through the bolted connection is determined.

Through analysis, it is found that the bolted connection structure can be regarded as a whole structure under reaching the critical preload, and the stiffness of the bolted structure will not change greatly. This way, the effect of connection stiffness on vibration transmission is explained.

**Table 7.** Differences in the vibration response between simulations and tests

		Exciting frequency [Hz]			
		24.4	100	150	200
Preload	2550 N	0.0%	-3.3%	-1.4%	0.8%
	4200 N	0.0%	-2.4%	-1.4%	0.8%
	6750 N	0.0%	-3.3%	-1.4%	0.8%

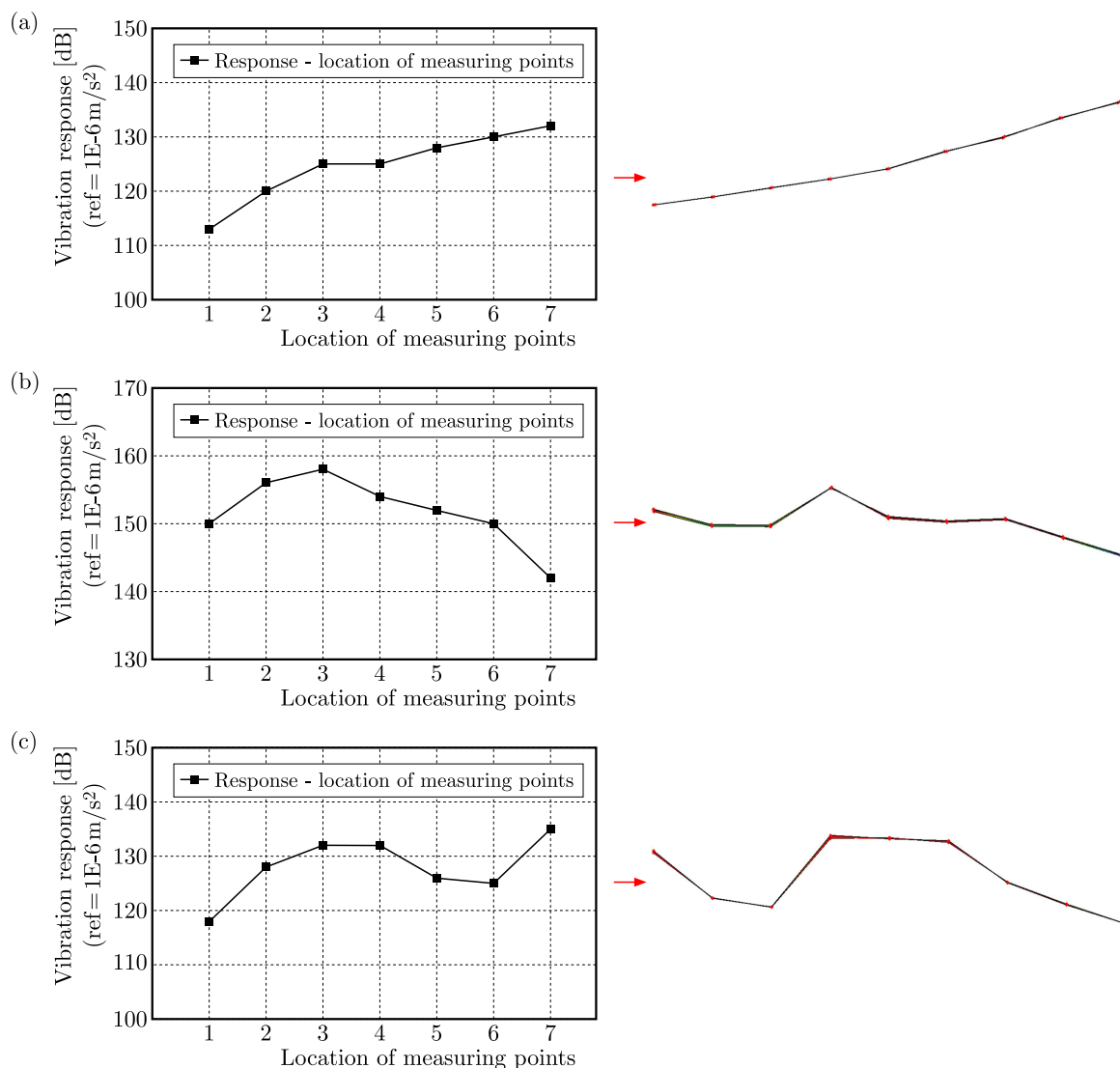


Fig. 12. The change trend of the response and mode (left: test vibration response; right: calculation mode): (a) first natural frequency, (b) second natural frequency, (c) third natural frequency

In order to verify validity of the calculation results, the trend of vibration response and vibration mode changes under the preload of 2550 N is compared. The natural frequency (1st-3rd) is as the exciting frequency. In Fig. 12, the displacement of modal nodes of natural frequencies

is consistent with the change trend of the forced vibration response at the same excitation frequency.

## 7. Conclusion

Two flat plates connected by bolts become a fixed overall structure, so their stiffness changes little with the friction coefficient, preload, temperature and internal pressure. The natural frequencies of each order increase with an increase of the friction coefficient, preload and pressure, and decrease with an increase of temperature, but the overall trend is not obvious (except for temperature). If the two flat plates connected by bolts cannot become a fixed overall structure, or the bolted structure fails, the stiffness of the structure will change.

At present, according to the calculation and test results, it can be seen that the connection stiffness is the main factor affecting the dynamic characteristics of the bolted connection structure. And various influencing factors studied in this paper will be examined further. An appropriate simulation method for the bolt connection based on the actual situation can be adopted.

In this paper, only two simple boundary conditions of bolted structures are studied. In the case of other boundary conditions, the effects of the friction coefficient, preload and temperature on the natural frequency of the structure need to be studied.

## References

1. DU Z., MI J., YAN W.F., 2018, Research on modeling method of dynamic contact stiffness of bolted joint, *Journal of Beijing Information Science and Technology University*, **33**, 2, 86-91
2. HAO Y., WANG J.L., LIU B., SUN H.C., HAN Y.H. CHEN F., 2021, Modal analysis theory and engineering application, *Journal of Hebei Institute of Architecture and Civil Engineering*, **3**, 4-47
3. LI J.F., YANG T., DU Y., NIU X.J., 2017, Composite laminates vibration theory and experimental modal analysis based on hammering method, *Aerospace Materials and Technology*, **47**, 1, 25-28+36
4. ROGERS P.F., BOOTHROYD G., 1975, Damping at metallic interfaces subjected to oscillating tangential loads, *Journal of Engineering for Industry*, **97**, 3, 1087-1093
5. SHEN P., NIU T.Y., CHEN J.Y., 2020, A comparative study on modal analysis and testing technology of cantilever beam, *Journal of Xinxiang University*, **9**, 54-56
6. TULLINI N., LAUDIERO F., 2008, Dynamic identification of beam axial loads using one flexural mode shape, *Journal of Sound and Vibration*, **318**, 1-2, 131-147